JACC: CARDIOVASCULAR IMAGING VOL. 6, NO. 1, 2013

PUBLISHED BY ELSEVIER INC. ISSN 1936-878X/$36.00

iMAIL

LETTERS TO THE EDITOR

CMR-Verified Interstitial Myocardial Fibrosis as a Marker of Subclinical Cardiac Involvement in *LMNA* Mutation Carriers

Lamin A/C (*LMNA*) gene mutation, identified in 10% of familial dilated cardiomyopathy (DCM) patients, is associated with an increased risk of sudden cardiac death (SCD), which may be the first clinical manifestation (1). Myocardial fibrosis (MF) has been identified in the hearts of *LMNA* mutation carriers experiencing arrhythmias or conduction disturbances, irrespective of left ventricular (LV) dilation and/or dysfunction (2). Thus, MF may be a precocious primary phenomenon responsible for the subsequent development of electrical instability and LV dysfunction. Cardiovascular magnetic resonance (CMR) allows the depiction of gross MF by late gadolinium enhancement (LGE), whereas extracellular/extravascular volume (ECV) fraction of the myocardium by pre- and post-contrast T1 mapping was recently demonstrated to detect interstitial MF (3). We aimed to investigate the incidence and pattern of MF using comprehensive CMR in *LMNA* mutation carriers.

We prospectively studied 7 families whose probands with the DCM phenotype were referred to our hospital between 2009 and 2011. We found 5 missense, 1 frame, and 1 splicing mutations (Online Appendix). All *LMNA* mutation carriers underwent biohumoral assays (hematocrit, N-terminal pro–B-type natriuretic peptide, plasma catecholamine, aldosterone, and plasma renin activity [PRA]), 12-lead electrocardiography, 24-h Holter monitoring, a cardiopulmonary exercise test, and CMR. All 6 probands received beta-blocker and/or an angiotensin-converting enzyme inhibitor therapy. A group of 16 age-matched healthy volunteers without a clinical history of cardiovascular disease was recruited as controls and underwent CMR, 12-lead electrocardiography, and blood sampling for hematocrit determination.

Participants were examined by 1.5-T unit (CVi, GE-Healthcare, Milwaukee, Wisconsin). Standard protocols for LV volume and function and late gadolinium enhancement (LGE) were performed. For myocardial ECV determination, T1 values of myocardium and blood cavity were measured in a single mid ventricular short-axis slice using modified-cine inversion-recovery sequence before and at fixed time intervals (5, 10, and 15 min) after a bolus of contrast agent (Gadodiamide-OMNISCAN,0.2 mmol/kg). Protocols, sequence parameters, T1-mapping, and myocardial ECV calculation are detailed in the Supplemental Material.

Baseline characteristics of *LMNA* mutation carriers and healthy controls are outlined in Tables 1 and 2, respectively. *LMNA* mutation carriers and healthy controls showed comparable age (46 ± 18 vs. 45 ± 13 years, $p = 0.717$) and body mass index (23.4 ± 4.1 vs. 24.0 ± 3.9 kg/m^2, $p = 0.659$), although a lower prevalence of male sex was observed in *LMNA* mutation carriers compared with healthy controls (37% vs. 75%, $p = 0.042$). *LMNA* mutation carriers had slightly larger LV end-diastolic volume and lower ejection fraction than healthy controls (87 ± 20 vs. 76 ± 12 ml/m^2 and 60 ± 8% vs. 68 ± 5%, respectively; both $p < 0.05$) (Online Fig. 1).

Five (26%) *LMNA* mutation carriers with an enlarged and dysfunctional left ventricle were older (67 ± 8 vs. 39 ± 14 years) and had a higher pro–B-type natriuretic peptide level (median 333 ng/l [25th to 75th percentiles: 62 to 1,943] vs. median 66 ng/l [25th to 75th percentiles: 29 to 107]) than *LMNA* mutation carriers with normal LV dimension and function (both $p < 0.05$). In all *LMNA* mutation carriers, PRA and catecholamine levels were within normal range, whereas the plasma aldosterone level was close to the upper normal limit (median 140 pg/ml [25th to 75th percentiles: 75 to 170], reference values: 20 to 180 pg/ml). Eight *LMNA* mutation carriers (42%) showed myocardial LGE with a patchy ($n = 3$) or mid wall ($n = 5$) pattern. In *LMNA* mutation carriers, LGE was more frequently detected in carriers with LV dysfunction (4 of 5 patients, 80%) compared with those with normal LV dimension and function (4 of 14 [29%], $p < 0.05$). Myocardial LGE was more common in carriers with first-degree atrioventricular block (4 of 5 [80%]) than those with normal atrioventricular conduction (1 of 14 [7%], $p < 0.05$).

Myocardial ECV was higher in *LMNA* mutation carriers than healthy controls (28.0 ± 2.9% vs. 22.7 ± 3.0%, $p < 0.001$) even after excluding LV segments with LGE (27.9 ± 3.7% vs. 22.7 ± 3.5%; $p < 0.001$). Myocardial ECV remained higher in *LMNA* mutation carriers after excluding carriers with LGE (28.6 ± 3.2% vs. 22.7 ± 3.5%, $p < 0.001$) or overt LV dysfunction (28.6 ± 2.9%, $p < 0.001$) (Online Fig. 1).

We demonstrated that interstitial MF represents a subclinical marker of cardiac involvement in genotype-positive *LMNA* carriers, likely determined by the expression of the mutated gene. This was substantiated by the fact that *LMNA* mutation carriers showed increased myocardial ECV than healthy controls also when the analysis was confined to carriers without LV dysfunction, electrical abnormalities, or LGE. Additionally, in *LMNA* mutation carriers, the PRA and aldosterone levels were not significantly increased, indicating that interstitial MF was unlikely related to the activation of the renin-angiotensin-aldosterone axis. These findings are concordant with previous studies reporting that *LMNA* mutation is

Table 1. Baseline Characteristics of *LMNA* Mutation Carriers

Case	Sex, M/F	Age, yrs	BMI, kg/m^2	CPK, U/l (rv <270)	NT-proBNP ng/l (rv <157)	Surface ECG	24-h Holter Lown class* (1–5)	LVEF, %	Peak Vo_2 ml/min/kg	Comorbidities
1 Proband	M	62	24.2	62	333	SR, AVB, LBBB	4a	49	24.1	Dyslip
2 Proband	M	76	22.3	91	943	SR, AVB, LBBB	4b	49	23.7	HT
3 Proband	F	67	28.3	95	81	SR	1	54	18.1	
4 Proband	F	74	22.7	72	3023	SR, AVB, LBBB	4b (SVT)	51	—	Dyslip
5 Proband	M	58	24.1	350	91	SR, AVB	4b (SVT)	56	24.2	
6 Proband	F	43	24.5	50	533	SR, LAFB	4b (SVT)	58	15	
7 Relative	M	57	30.3	135	42	SR	4b	52	24.9	Dyslip
8 Relative	M	39	24.1	129	25	SR	1	58	41	
9 Relative	F	43	17.7	53	13	SR	1	75	33.7	
10 Relative	M	35	23.6	172	64	SR, AVB	4b	70	33.6	
11 Relative	F	28	20.5	70	72	SR	1	60	38.5	
12 Relative	F	43	20.8	72	50	SR	0	61	21.9	
13 Relative	F	13	19.1	88	30	SR	0	71	26.3	
14 Relative	F	64	32.5	77	101	SR	1	67	20.6	Dyslip,HT
15 Relative	M	33	28.4	487	12	SR	1	67	29.3	
16 Relative	F	38	18.9	290	124	SR	4b	62	28.2	
17 Relative	F	51	22.0	66	266	SR	1	66	27.2	
18 Relative	F	41	23.6	112	68	SR	4a	60	23.9	
19 Relative	F	18	17.7	70	43	SR	1	57	29	

*Lown classification of ventricular arrhythmias: isolated monomorphic ventricular beats <720/d (class 1), >720/d (class 2), isolated polymorphic ventricular beats (class 3), ventricular couplets (class 4a), ventricular tachycardias (class 4b), ventricular beats with R/T phenomenon (class 5); patients with sustained ventricular tachycardia are indicated.
AVB = first-degree atrioventricular block; BMI = body mass index; CPK = creatine phosphokinase; ECG = electrocardiogram; Dyslip = dyslipidemia; F = female; HT = hypertension; LAFB, left anterior fascicular block; LBBB = left bundle branch block; LVEF, left ventricular ejection fraction by cardiovascular magnetic resonance; M = male; NT-proBNP = N-terminal pro–B-type natriuretic peptide; rv = range value; SR = sinus rhythm; SVT = sustained ventricular tachycardia; Vo_2 = peak oxygen consumption.

associated with myocardial and skeletal muscle fibrosis (2), indicating that MF may occur as primary phenomenon due to mutated gene expression. On the other hand, myocardial LGE was more common in carriers with LV dysfunction and/or electrical disturbances rather representing an unspecific marker of myocardial damage (4).

In conclusion, CMR showed that MF is an intrinsic feature of *LMNA* cardiomyopathy ranging from interstitial to gross MF. Interstitial MF may represent a subclinical marker preceding the overt structural, functional, and electrical abnormalities. In contrast, gross MF is more commonly detected in carriers already expressing the typical cardiac phenotype.

Table 2. Baseline Characteristics of Healthy Controls

Case	Sex M/F	Age, yrs	BMI, kg/m^2	Surface ECG	LVEF, %	Comorbidities
1 Control	F	34	17.9	SR	66	
2 Control	M	72	26.6	SR	71	Mild COPD
3 Control	M	21	22.8	SR	78	
4 Control	M	61	25.7	SR	79	
5 Control	M	29	20.8	SR	68	
6 Control	M	51	19.6	SR	71	
7 Control	F	28	24.2	SR	72	
8 Control	M	36	19.8	SR	64	
9 Control	M	46	33.3	SR	65	
10 Control	M	51	27.4	SR	65	
11 Control	M	40	25.1	SR	70	
12 Control	M	40	25.9	SR	62	
13 Control	F	46	19.3	SR	72	
14 Control	F	63	26.3	SR	68	Mild COPD
15 Control	M	50	23.5	SR	61	
16 Control	M	45	26.4	SR	66	

COPD = chronic obstructive pulmonary disease; other abbreviations as in Table 1.

Marianna Fontana, MD, Andrea Barison, MD, Nicoletta Botto, PhD, Luca Panchetti, MD, Giulia Ricci, MD, Matteo Milanesi, PhD, Roberta Poletti, MD, Vincenzo Positano, MSc, Gabriele Siciliano, MD, PhD, Claudio Passino, MD, PhD, Massimo Lombardi, MD, Michele Emdin, MD, PhD, Pier Giorgio Masci, MD*

*Fondazione CNR/Regione Toscana G. Monasterio, Via Giuseppe Moruzzi 1, 56124 Pisa, Italy. *E-mail: masci@ftgm.it.*

http:dx.doi.org/10.1016/j.jcmg.2012.06.013

Please note: Drs. Fontana and Barison contributed equally to this paper.

REFERENCES

1. Van Berlo JH, Voogt WG, Kooi AJ, et al. Meta-analysis of clinical characteristics of 299 carriers of *LMNA* gene mutations. J Mol Med 2005;83:79–83.
2. Van Tintelen JP, Tio RA, Kerstjens-Frederikse WS, et al. Severe myocardial fibrosis caused by a deletion of the 5′ end of lamin A/C gene. J Am Coll Cardiol 2007;49:2430–9.
3. Jerosch-Herold M, Sheridan DC, Kushner JD, et al. Cardiac magnetic resonance imaging of myocardial contrast uptake and blood flow in patients affected with idiopathic or familial dilated cardiomyopathy. Am J Physiol Heart Circ Physiol 2008;295:H1234–42.
4. Raman SV, Sparks EA, Baker PM, et al. Mid-myocardial fibrosis by cardiac magnetic resonance in patients with lamin A/C cardiomyopathy. J Cardiovasc Magn Reson 2007;9:907–13.

▶APPENDIX

For supplemental material, please see the online version of this article.

Lipid-Rich Versus Fibrous Intimal Hyperplasia in Transplant Vasculopathy*

In the June 2012 issue of *iJACC*, Hou et al. (1) reported that the optical coherence tomography (OCT), compared with intravascular ultrasound (IVUS), was more sensitive for early detection of cardiac allograft vasculopathy (CAV). Mean intimal hyperplasia (IH) was 180 μm. IH thickness <150 μm accounted for 31% of assessable segments, which is underresolution of IVUS. Lipid-rich plaques (LCPs) with thin fibrous caps were found by OCT in 43% of transplant recipients.

The incidence of CAV is as high as 50% at 5 years after transplantation, and survival is substantially curtailed after the diagnosis of CAV is established. Despite the significant progress in the control of cellular rejection, the evolution of graft vasculopathy has continued unabated. Aggressive control of established risk factors and some of the newer antiproliferative agents remain the cornerstone of CAV management. Use of statins has demonstrated an outcome benefit by cholesterol reduction and also by the cholesterol-independent immune-modulating effect on the natural killer cells; the immunomodulatory efficacy of statins is exaggerated in the presence of a calcineurin inhibitor (2).

We need to use sensitive tools for the diagnosis and screening of CAV to develop novel treatment strategies. Due to the denervation of transplanted hearts, symptoms of vasculopathy are usually not obvious. Therefore, coronary angiography is repeated annually in most transplantation centers. However, information obtained from angiography is often limited because CAV is diffuse. IVUS is able to accurately image the 3 vessel wall layers, and the IH evaluation by IVUS correlates with the occurrence of adverse events post-transplantation. IH of >500 μm in the first year after transplantation predicts increased mortality, myocardial infarction, and late development of severe CAV and heart failure (3). Further differentiation of fibrous from lipid-rich neointima offers a significant prognostic and therapeutic advantage. Although gray-scale IVUS is unable to determine the etiology of CAV, intravascular OCT generates cross-sectional vessel images with 10-fold higher resolution than IVUS and with a more precise characterization of IH. Assessment of lipid-rich lesions is also possible by near-infrared spectroscopy (NIRS), in which the NIRS measurements are presented as a chemogram with the probability of a lipid core containing plaques on a color scale from red to yellow (0 for red, 1 for

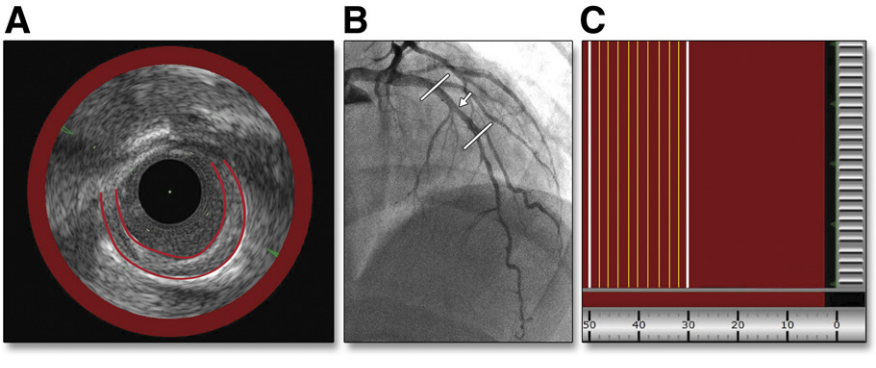

Figure 1. Diffuse Cardiac Allograft Vasculopathy

Intravascular ultrasound (IVUS) **(A)**, angiography **(B)**, and near-infrared spectroscopy (NIRS) **(C)** scans of the medial left anterior descending artery (LAD) in an 18-year-old male patient 11 years after heart transplantation for dilated cardiomyopathy. The **white arrow (B)** indicates the location of the presented IVUS cross-sectional image. **White lines (B and C)** represent a region of the angiogram corresponding to the NIRS scan. **Yellow lines (C)** represent 2-mm blocks. The patient received immunosuppressive therapy with lipid-lowering agents (tacrolimus, prednisone, mycophenolate, aspirin, and simvastatin). Coronary angiography showed diffuse disease especially prominent in the mid LAD. Pruning of the secondary and tertiary coronary vasculature is evident. IVUS minimal lumen area = 4.5 cm^2, and NIRS chemogram lipid core burden index = 0.